

Testing the Modified Press–Schechter Model against N-Body Simulations

Andreu Raig¹, Guillermo González-Casado² and Eduard Salvador-Solé¹

¹*Departament d’Astronomia i Meteorologia, Universitat de Barcelona, Martí Franquès 1, E-08028 Barcelona, Spain*

²*Departament de Matemàtica Aplicada II, Universitat Politècnica de Catalunya, Pau Gargallo 5, Edifici U, E-08028 Barcelona, Spain*

7 February 2020

ABSTRACT

A modified version of the extended Press–Schechter model for the growth of dark-matter haloes was introduced in two previous papers with the aim at explaining the mass-density relation shown by haloes in high-resolution cosmological simulations. In this model major mergers are well separated from accretion, thereby allowing a natural definition of halo formation and destruction. This makes it possible to derive analytic expressions for halo formation and destruction rates, the mass accretion rate, and the probability distribution functions of halo formation times and progenitor masses. The stochastic merger histories of haloes can be readily derived and easily incorporated into semi-analytical models of galaxy formation, thus avoiding the usual problems encountered in the construction of Monte Carlo merger trees from the original extended Press–Schechter formalism. Here we show that the predictions of the modified Press–Schechter model are in good agreement with the results of N -body simulations for several scale-free cosmologies.

Key words: cosmology – dark matter – galaxies: formation, evolution

1 INTRODUCTION

The last decade saw the significant development of semi-analytical techniques used to model galaxy formation in hierarchical cosmologies (e.g., Lacey et al. 1993; Kauffmann, White & Guiderdoni 1993; Cole et al. 1994; Nuslen & Fabian 1997; Avila-Reese & Firmani 1998; Cavaliere, Menci & Tozzi 1999; Somerville & Primack 1999; Cole et al. 2000). The prediction of the merger histories of dark-matter haloes is fundamental to all these techniques. Some recent schemes extract halo evolution directly from cosmological N -body simulations (Roukema et al. 1997; van Kampen, Jiménez & Peacock 1999; Kauffmann et al. 1999). However, the most popular semi-analytical models (SAMs) use Monte Carlo simulations of halo merger histories, the so-called merger trees (e.g., Kauffmann et al. 1993; Somerville & Primack 1999; Cole et al. 2000) derived from the framework of the extended Press–Schechter (EPS) theory (Bower 1991; Bond et al. 1991; Lacey & Cole 1993, hereafter LC93).

Despite its simplicity, the EPS theory has proved to be a very powerful tool to model the merger histories of dark-matter haloes. The predicted halo mass function is consistent with the results of N -body simulations. Although there are significant discrepancies at some redshifts (e.g., Gross et al. 1998; Tormen 1998; Somerville et al. 2000), they can be conveniently dealt with by means of different corrections (Lee & Shandarin 1998; Sheth & Tormen 1999; Jenkins et al. 2001; Sheth, Mo & Tormen 2001). Furthermore, detailed comparisons with N -body simulations indicate that the EPS theory provides a reliable statistical description of halo evolution (Kauffmann & White 1993; Lacey & Cole 1994, hereafter LC94; Somerville et al. 2000).

However, several issues concerning the practical implementation of merger trees from the EPS theory require further study (see Somerville & Kolatt 1999; Somerville et al. 2000; Cole et al. 2000):

(i) The number (although not the mass) of progenitors of a halo diverges for progenitor masses approaching zero. Therefore it is necessary to introduce a minimum mass cut-off, or mass resolution, when constructing Monte Carlo merger trees to avoid infinite ramification. The problem is then how to account in a self-consistent way for the mass enclosed within unresolved haloes.

(ii) To select the masses of resolved progenitors, one uses the conditional probability (provided by the EPS model) that a halo of a given mass at a given time has a progenitor of a smaller mass in an earlier epoch. However, this probability

corresponds to *one single object* which implies that, having found one progenitor of a given mass, it cannot be used to find the mass of another progenitor. This introduces great uncertainties, namely, there is no way to decide how many progenitors above the resolution to consider nor the total mass that must be assigned to them.

(iii) In merger trees, the branching of haloes into their resolved progenitors is imposed in a set of individual times which are separated by an arbitrary step, i.e., there is also some time resolution. Progenitor mergers are then identified with these time-sparse merger nodes while they actually take place at some unknown moment between them.

Several ways have been proposed to enforce mass conservation in merger nodes and simultaneously reproduce the conditional mass function of the EPS theory (Kauffmann & White 1993; LC93; LC94; Kitayama & Suto 1996; Somerville & Kolatt 1999; Somerville et al. 2000; Cole et al. 2000). However, no fully satisfactory solution has been found to date. For example, recent methods use non-arbitrary time steps (Somerville & Kolatt 1999; Cole et al. 2000), but the caveat always remains that true mergers do not take place at the merger nodes where progenitors are identified. In fact, the latter problem will always be found in the EPS model because of its lack of a clear characterization of halo formation and destruction.

LC93 introduced a prescription to characterize the formation and destruction of haloes in the EPS model. The formation time is defined as the time when half the halo mass is assembled into a single progenitor. Likewise, the destruction time is defined as the time when the halo doubles in mass. However, such definitions do not account for the way mass is assembled. No distinction is made, for example, between a halo which has increased its mass through one single capture of another similar massive halo and one which has increased its mass through consecutive captures of very small relative mass haloes. A more realistic characterization of the formation and destruction of haloes should account for this distinction. Only major mergers are expected to produce, through violent relaxation, a substantial rearrangement of the structure of haloes. Consequently, major mergers can be regarded as causing the formation of new haloes with *distinct* structural properties from the original ones which are destroyed in the event. In contrast, minor mergers do not produce significant disturbances in the equilibrium state and the structure of the massive partner experiencing them. They simply cause a smooth mass increase, which is commonly called accretion. Hence, in minor mergers, the identity of the capturing halo with *essentially unaltered* structural properties prevails.

Salvador-Solé, Solanes & Manrique (1998, hereafter SSM) introduced the minimal self-consistent modification of the EPS model which incorporates the previous natural definitions of halo formation and destruction. In this new model, hereafter referred to as the modified Press–Schechter (MPS) model, the distinction between major and minor mergers is made through a phenomenological frontier Δ_m in the fractional mass captured by a halo. Captures above this threshold are taken to be major mergers, while those below are considered minor mergers which contribute to accretion. SSM found that, given an effective value of Δ_m of about 0.5–0.7, the empirical mass-density relation shown by haloes in high resolution N -body simulations of distinct hierarchical cosmologies (Navarro, Frenk & White 1997, hereafter NFW) is naturally reproduced under the assumption proposed by NFW that the characteristic density of haloes is proportional to the critical density of the universe at the time of their formation. Raig, González-Casado & Salvador-Solé (1998, hereafter RGS) subsequently showed that the mass-density relation is, in this case, not only consistent with, but actually implied by the MPS model. To prove this, RGS assumed haloes endowed with a universal density profile à la NFW. However, the same conclusion holds whatever the form of the halo density profile (González-Casado, Raig & Salvador-Solé 1999). More importantly, using the MPS model, Manrique, Salvador-Solé & Raig (2001) have recently shown that the true shape à la NFW of halo density profiles is the natural consequence of hierarchical clustering.

Hence, the MPS model provides a consistent description of both the growth history and the internal structure of haloes. Furthermore, as shown here, the MPS model overcomes the problems encountered with Monte Carlo merger trees built from the EPS model (see also Salvador-Solé et al. 2001). The ability of the MPS model to account for the structure of dark-matter haloes strongly supports its validity. However, before incorporation into a SAM of galaxy formation the MPS model should be thoroughly tested against cosmological N -body simulations, as was the EPS model (e.g., LC94). This is the aim of the present paper. In particular, we propose to check the correct behaviour of all quantities predicted by the MPS model that represent a novelty over the original EPS model, namely, the rates of halo formation and destruction, the mass accretion rate, and the probability distribution functions (PDFs) of halo formation times and progenitor masses.

In Section 2 we review the MPS model. In Section 3 we describe the N -body simulations used to test the model and the way the empirical quantities have been extracted from them. The comparison between theory and simulations is presented in Section 4 and the main results of this comparison summarized in Section 5.

2 THE MPS MODEL

Press & Schechter (1974) derived, in a rather heuristic manner, the simple expression

$$N(M, t) dM = \left(\frac{2}{\pi}\right)^{1/2} \frac{\rho_0}{M^2} \frac{\delta_c(t)}{\sigma(M)} \left| \frac{d \ln \sigma}{d \ln M} \right| \exp \left[-\frac{\delta_c^2(t)}{2\sigma^2(M)} \right] dM \quad (1)$$

for the mass function of haloes in a hierarchical universe endowed with Gaussian random initial density fluctuations. In equation (1), $N(M, t) dM$ gives the comoving number density of haloes with masses in the range M to $M + dM$ at time t , $\delta_c(t)$ is the linear extrapolation to the present time t_0 of the critical overdensity for collapse at t , $\sigma(M)$ denotes the r.m.s. mass fluctuation of the linear extrapolation to t_0 of the density field smoothed over spheres of mass M , and ρ_0 is the current mean density of the universe.

A more rigorous derivation of the Press–Schechter mass function (including the correct normalization factor) was provided by Bond et al. (1991) who also inferred the conditional mass function (see also Bower 1991). Their theory was subsequently extended by LC93, who derived the conditional probability that a halo with M at t ends up within a halo of a larger mass between M' and $M' + dM'$ at a later time t' . By taking the limit of the latter conditional probability for t' tending to t , LC93 also obtained the instantaneous halo merger rate,

$$r_{\text{LC}}^{\text{m}}(M \rightarrow M', t) dM' = \left(\frac{2}{\pi}\right)^{1/2} \frac{1}{\sigma^2(M')} \left| \frac{d\delta_c}{dt} \frac{d\sigma(M')}{dM'} \right| \frac{1}{[1 - \sigma^2(M')/\sigma^2(M)]^{3/2}} \times \exp \left\{ -\frac{\delta_c^2(t)}{2} \left[\frac{1}{\sigma^2(M')} - \frac{1}{\sigma^2(M)} \right] \right\} dM', \quad (2)$$

which provides the fraction of the total number of haloes with M at t which give rise, per unit time, to haloes with masses between M' and $M' + dM'$ through instantaneous mergers.

2.1 Growth rates

In the MPS model the distinction made between major and minor mergers does not affect the number density of haloes present at any time. This is therefore given by the Press–Schechter mass function (eq. [1]). However, this distinction substantially modifies the description of halo growth.

The instantaneous *major* merger rate is defined in the same way as the Lacey–Cole merger rate (eq. [2]) but is restricted to mergers above the threshold Δ_{m} ,

$$r^{\text{m}}(M \rightarrow M', t) dM' = r_{\text{LC}}^{\text{m}}(M \rightarrow M', t) \theta[M' - M(1 + \Delta_{\text{m}})] dM'. \quad (3)$$

with $\theta(x)$ the Heaviside step function.

Note that, due to the divergent abundance of small mass haloes that can be captured, the Lacey–Cole merger rate $r_{\text{LC}}^{\text{m}}(M \rightarrow M', t) dM'$ diverges for $M' - M$ tending to zero (see eq. [2]) while the major merger rate defined in equation (3) does not have such a divergence.

The integral of this instantaneous major merger rate over the range of final halo masses gives the rate at which haloes with M at t are destroyed because of major mergers, i.e., the instantaneous halo destruction rate,

$$r^{\text{d}}(M, t) = \int_M^\infty r^{\text{m}}(M \rightarrow M', t) dM'. \quad (4)$$

From the major merger rate one can define a useful related quantity, the instantaneous capture rate, which gives the fraction of the total number of haloes with M' at t that arise, per unit time, from the capture with destruction of haloes with smaller masses between M and $M + dM$,

$$r^{\text{c}}(M' \leftarrow M, t) dM \equiv r^{\text{m}}(M \rightarrow M', t) \frac{N(M, t)}{N(M', t)} dM = r_{\text{LC}}^{\text{m}}(M \rightarrow M', t) \theta[M' - M(1 + \Delta_{\text{m}})] \frac{N(M, t)}{N(M', t)} dM' \quad (5)$$

Note that captured haloes with $M > M'/(1 + \Delta_{\text{m}})$ do not contribute to this expression because these massive haloes are not destroyed in the capture and evolve into M' by accretion.

The instantaneous formation rate, i.e., the rate at which haloes with M' form at t via major mergers, is given by half the integral of the instantaneous capture rate over the range of captured haloes more massive than $M' \Delta_{\text{m}}/(1 + \Delta_{\text{m}})$,

$$r^{\text{f}}(M', t) = \frac{1}{2} \int_{M' \Delta_{\text{m}}/(1 + \Delta_{\text{m}})}^{M'} r^{\text{c}}(M' \leftarrow M, t) dM. \quad (6)$$

Indeed, captures with destruction of haloes less massive than $M' \Delta_{\text{m}}/(1 + \Delta_{\text{m}})$ do not contribute to the formation of new haloes. The capture of one single halo of that mass is not enough to cause the destruction of the capturing halo, while the simultaneous capture of a large number, giving rise to a substantially more massive halo than the capturing one and thereby producing its destruction, is extremely improbable. (The validity of this argument is confirmed a posteriori.) Therefore, to ensure the formation of new haloes, captures must involve at least one halo which is more massive than $M' \Delta_{\text{m}}/(1 + \Delta_{\text{m}})$.

But then haloes with masses between $\Delta_m M'/(1 + \Delta_m)$ and $M'/2$ will be captured by haloes with masses essentially in the complementary range from $M'/2$ to $M'/(1 + \Delta_m)$, and conversely. Therefore, to estimate the halo formation rate captures must be counted in only one of these ranges. The two possible estimates corresponding to each range give essentially the same result in the three cosmologies analysed. We found no difference in the $n = 0$ case and a constant difference of 1.6 % and 0.6 % in the $n = -2$ and $n = -1$ cases, respectively. A slightly better estimate, adopted in expression (6), is still provided by the arithmetic mean of both estimates.

The validity of binary approximation used in the previous reasoning is shown not only by the similarity between the two alternative estimates of the formation rate, but mainly by the shape of the capture rate in the range $M' \Delta_m / (1 + \Delta_m) < M < M' / (1 + \Delta_m)$: this function is very nearly symmetric around $M'/2$ (see Fig. 1). It must be emphasized that in the present theory the formation of a new halo is an instantaneous event that corresponds to the capture by some predecessor of a similar massive object. This massive capture is clearly less probable than the capture of a less massive object. It is therefore understood that halo formation corresponds to rare binary mergers between similar massive haloes while accretion corresponds to much more frequent, often multiple, minor mergers.

In the MPS model, the total mass increase rate of haloes with M at t splits into two contributions, one due to major mergers and the other to accretion. Here, we are particularly concerned with the latter. The instantaneous mass accretion rate, i.e., the rate at which haloes with M at t increase their masses due to minor mergers, is

$$r_{\text{mass}}^{\text{a}}(M, t) = \int_M^{M(1+\Delta_m)} (M' - M) r_{\text{LC}}^{\text{m}}(M \rightarrow M', t) dM'. \quad (7)$$

This rate, as with all preceding ones, is intended to globally characterize haloes with M at t . It measures the *expectation value*, for any halo, of the instantaneous mass increase rate due to minor mergers, or equivalently, by the ergodicity condition, the *average* of the real instantaneous mass increase rate due to minor mergers over all these haloes. Nevertheless, since accretion is a very common event involving a number of relatively small mass haloes, equation (7) should also provide a reasonable approximation for the true instantaneous mass increase rate experienced by any halo with M at t due to accretion. Consequently, the solution of the differential equation

$$\frac{dM(t)}{dt} = r_{\text{mass}}^{\text{a}}[M(t), t], \quad (8)$$

with $M(t_i) = M_i$, giving the *mean* $M(t)$ trajectory followed between two major mergers by haloes with M_i at t_i , should also be a reasonable approximation for the true $M(t)$ track followed by any halo. For this reason, we shall call this “the theoretical accretion track”. The validity of this approximation will be checked in Section 4.2.

It can be argued that in the MPS model the parameter Δ_m plays the same role as the mass resolution used in the EPS model when building Monte Carlo merger trees and that, in the present model, the formation of new haloes through binary major mergers between similarly massive haloes plays the same role as merger nodes in the Monte Carlo simulations. In both cases only captures above some mass cut-off are seen as true mergers while those below it are regarded as contributing to accretion. However, the potential of the MPS model to solve the problems mentioned in Section 1 does not rely on this distinction alone, but also on the new definitions of halo destruction and formation that accompany it. In the MPS model there are haloes which are destroyed or formed at the exact moment in which they are analysed. Therefore, it is possible to define and derive the instantaneous destruction and formation rates (eqs. [4] and [6]) with no counterpart in the EPS model and, from them (see next subsections), the PDFs of formation and destruction times and of progenitor masses that solve problems (ii) and (iii). Furthermore, because halo formation takes place at definite times in which the progenitors and the newly formed haloes coincide, we can identify such events as *true* merger nodes. Finally, the mass increase of a halo due to the cumulative effect of minor mergers that occur at any time after its formation is consistently taken into account in the MPS model through the instantaneous mass accretion rate (eq. [7]) or the theoretical accretion track derived from it (eq. [8]) which also solves problem (i).

2.2 Formation times

To derive the PDF of halo formation times we shall assume that the mass evolution $M(t)$ of a halo since the last major merger that gave rise to it is well described by the theoretical accretion track (eq. [8]). In this case, the cumulative number density of haloes at t_i with masses in the arbitrarily small range M_i to $M_i + \delta M_i$ which pre-exist at an early time $t < t_i$, i.e., the spatial number density of haloes which evolve by accretion from t to t_i ending up with a mass between M_i and $M_i + \delta M_i$ is (Manrique & Salvador-Solé 1996; Manrique et al. 1998)

$$N_{\text{pre}}(t) = N[M_i, t_i] \delta M(t) \exp \left\{ - \int_t^{t_i} r^{\text{f}}[M(t'), t'] dt' \right\}, \quad (9)$$

where

$$\delta M(t) = \delta M_i \exp \left[- \int_t^{t_i} \frac{\partial r_{\text{mass}}^a(M, t')}{\partial M} \Big|_{M=M(t')} dt' \right] \quad (10)$$

is the mass element at t that evolves into δM_i at t_i following theoretical accretion tracks. Therefore, the PDF of formation times for haloes with masses between M_i and $M_i + \delta M_i$ at t_i is given by

$$\Phi_f(M_i, t) \equiv \frac{1}{N_{\text{pre}}(t_i)} \frac{dN_{\text{pre}}}{dt} = r^f[M(t), t] \exp \left\{ - \int_t^{t_i} r^f[M(t'), t'] dt' \right\}, \quad (11)$$

where $N_{\text{pre}}(t_i) = N(M_i, t_i)$. The median for this distribution defines the typical formation time t_f of haloes with M_i at t_i . This follows from the usual definition that the typical formation time of a population is the epoch in which its abundance was a factor e smaller. Similarly (see Manrique & Salvador-Solé 1996 and Manrique et al. 1998), one can derive the PDF of halo destruction times and the associated typical destruction time t_d . Finally, the typical survival time of haloes with M_i at t_i is taken as the difference $t_d - t_i$.

In estimating the mass evolution of haloes between major mergers by means of their theoretical accretion tracks we neglect the diffusion of true accretion tracks (in the mass vs. time diagram) caused by random minor mergers. Were this diffusion negligible or exactly symmetric with regard to the mean $M(t)$ trajectory given by the theoretical accretion track, the following conservation equation of the number density of haloes per unit mass along accretion tracks would be satisfied

$$\frac{d \ln N(M, t)}{dt} + \frac{\partial r_{\text{mass}}^a(M', t)}{\partial M'} \Big|_{M'=M} - r^f(M, t) + r^d(M, t) = 0. \quad (12)$$

This conservation equation was used by SSM (suggested by Manrique et al. 1998) to derive the formation rate from quantities $N(M, t)$, $r_{\text{mass}}^a(M', t)$, and $r^d(M, t)$. Note that this estimate of the formation rate alternative to equation (6) is independent of the binary major merger approximation but may be affected, in turn, by any asymmetric diffusion of accretion tracks. Since binary approximation is very accurate, the comparison between these two alternative estimates of the formation rate provides quantitative information about the true asymmetry of diffusion.

In Figure 2 we show the absolute value of the relative difference between the two estimates of the formation rate (eqs. [6] and [12]) as a function of halo mass for several cosmologies. For large n there is good agreement at small masses but there is a significant deviation at large masses, while for small n the difference is rather insensitive to mass, although it is significant at all values. We conclude that the effects of diffusion cannot be neglected and, consequently, that the only reliable estimate of halo formation rate is given by equation (6). The effects of diffusion on the distribution of formation times (eq. [11]) is examined in Section 4.

2.3 Progenitor masses

Finally, the PDF of progenitor masses can be derived by taking into account that major mergers are essentially binary. Given a halo formed at t with mass M , the probability that the most massive or primary progenitor has a mass in the range M_1 to $M_1 + dM_1$ at t is given by

$$\begin{aligned} \Phi_p(M_1, M) dM_1 &\equiv \frac{r^c(M \leftarrow M_1, t)}{r^f(M, t)} dM_1 \\ &= 2 G(M_1, M) dM_1 \left[\int_{M \Delta_m / (1 + \Delta_m)}^{M / (1 + \Delta_m)} G(\tilde{M}, M) d\tilde{M} \right]^{-1} \end{aligned} \quad (13)$$

with

$$G(M', M) = \frac{1}{M' \sigma^2(M')} \left| \frac{d\sigma(M')}{dM'} \right| \left[1 - \frac{\sigma^2(M)}{\sigma^2(M')} \right]^{-3/2}. \quad (14)$$

In equation (13), M_1 takes values in the range between $M/2$ and $M/(1 + \Delta_m)$. The PDF for the mass M_2 of the secondary progenitor is given, in turn, by the same expression (13) but replacing M_1 by M_2 which takes values in the range $\Delta_m M / (1 + \Delta_m)$ to $M/2$. Since the capture rate is essentially symmetric around $M/2$ (see Fig. 1) the typical masses of the two progenitors can be computed by taking the median value M_1 for the distribution (13) of the primary progenitor and then the difference $M_2 = M' - M_1$ for the secondary one, or conversely. Notice that the PDFs of primary and secondary progenitor masses in the MPS theory are independent of time (see eqs. [13] and [14]).

The number and total mass of progenitors of a halo are fully determined in the present theory thanks to binary approximation. This approximation is amply justified by the shape of the instantaneous capture rate. Nonetheless, all predictions based on it will be carefully checked in Section 4. The same approximation is often used when constructing Monte Carlo merger trees from the EPS model. There is, however, an important difference between the two cases. In the MPS model, major mergers yielding the formation of new haloes involve only similar massive progenitors and occur effectively at the

formation time, while in the EPS model, mergers involve resolved progenitors of any mass ratio and can occur at any moment between two consecutive nodes of the merger tree. Therefore the validity of binary approximation is not so obvious in the latter case. Of course, one may enforce it by taking a small enough time step and a sufficiently large mass resolution, but this tends to reproduce the optimal conditions encountered, by construction, in the MPS model.

3 N-BODY SIMULATIONS

3.1 The data

To check that the behaviour of the MPS model is correct, we have used the outcome of the cosmological N -body simulations performed by LC94 and used by these authors to test the EPS model. Here we only provide a brief summary of the most relevant aspects of these simulations concerning the present work (see LC94 for a detailed description).

Simulated data correspond to three Einstein–de Sitter (i.e., $\Omega = 1$, $\Lambda = 0$) universes with a power-spectrum of initial density fluctuations given by a power law, $P(k) \propto k^n$, with spectral index n equal to -2 , -1 , and 0 . The simulations were performed using the P^3M code of Efstathiou et al. (1985) with 128^3 particles and a mesh of 256^3 points. The output times were selected so that the characteristic mass $M_*(t)$ increases by a factor of $\sqrt{2}$ between each pair of successive output times, where $M_*(t)$ is defined by the relation

$$\sigma[M_*(t)] = \delta_c(t) = \delta_c(t_0) \frac{a(t_0)}{a(t)}, \quad (15)$$

with $a(t)$ the expansion factor of the universe.

LC94 found good agreement between the analytical predictions of the EPS model, for $\delta_c(t_0) = 1.69$ and a top-hat filter (with smoothing scale R related with the filter mass through $M = \frac{4\pi}{3}\rho_0 R^3$), and the results of their simulations when haloes were selected by means of the conventional friends-of-friends algorithm with a dimensionless linking length of $b = 0.2$. In the present work, we use the same strategy to identify haloes from simulations. The same filtering window and the same value of the critical overdensity are also used to derive the theoretical predictions from the MPS model. LC94 found better fits to the *mass function* of simulated haloes when $\delta_c(t_0)$ was allowed to vary. In any event, the best-fit was obtained for a value which was still very close to the standard of 1.69. (Using this standard value LC94 found that the theoretical mass function overestimates the abundance of haloes in N -body simulations, particularly at the lower and higher mass ends, by a factor never exceeding 2; see Fig. 1 of LC94.)

In the three simulated scale-free universes the evolution of structure is *self-similar*. In this case one has

$$\sigma(M) \propto M^{-(n+3)/6}, \quad (16)$$

implying that $a(t)$ changes by a factor $2^{(n+3)/12}$ between each successive output time of the simulations. Consequently, the output time step for each individual simulation is constant in logarithmic scale, although it is longer in simulations with a larger value of n . As pointed out by LC94, the advantage of having self-similar universes is that objects identified at different times t but with the same value of the scaled mass $M(t)/M_*(t)$ are indistinguishable. Therefore we can normalize all masses M to the characteristic mass M_* at the corresponding time t and combine the results obtained from bins of identical normalized mass \tilde{M} for several output times, thereby drastically reducing the statistical noise in the empirical quantities derived from simulations.

3.2 Tracing halo evolution

Here we describe the general procedure that we followed to trace the past and future evolution of haloes present at a given output time in the simulations. The first practical problem encountered concerns the stability of haloes in simulations. As it is well known, halo-finding algorithms, such as the friends-of-friends technique, have several intrinsic shortcomings which may distort the evolution of simulated haloes: those particles that are close, although gravitationally unbound, to a halo may be assigned to it. Conversely, gravitationally bound particles may be excluded when their orbits have led them far from the identified halo region. To minimize these effects we followed LC94 and considered only haloes with at least 20 particles. Another difficulty is that the outcome of simulations is only saved at a discrete set of times t_k while the MPS theory deals with instantaneous major mergers that occur at definite times which do not coincide in general with any output time t_k . Since the most important quantities in the EPS theory refer to arbitrary time intervals this difficulty could be avoided in the LC94 study. Note, however, that this difference between the two studies does not reflect any shortcoming of the MPS model over the EPS theory, but simply that the former provides a finer description of the dark-matter aggregation process.

We must assess whether a halo with mass M at an output time t formed in a major merger that took place *after the previous output time* t' or has evolved by accretion (i.e., it has only experienced minor mergers) since then. Suppose we identify the halo M_1 at t' harbouring the largest number of particles which end up within M at t . We will call it the most massive

predecessor at t' of the halo M at t (not to confuse this with the primary progenitor). The theoretical threshold Δ_m applies in the case of t and t' infinitely close, while the masses M and M_1 refer to two distinct times. So even when $(M - M_1)/M$ is larger than Δ_m the evolution may have taken place by accretion. This is true when the remaining mass $M - M_1$ is distributed among many small lumps. On the other hand, even in the case of binary major mergers, the particles located in the final object M will not be found within only two haloes at t' : apart from the major merger, there is some accretion onto the two progenitors before the merger and onto the final halo after it. In other words, neither of these two simple criteria (i.e., the condition $(M - M_1)/M > \Delta_m$ and the location of the particles belonging to halo M in only two predecessors) can identify halo formation. For this reason, we applied an improved combination of both. Concretely, we took into account that major mergers yielding the formation of new haloes are binary events among coeval haloes that have increased their masses by accretion since t' up to the merger time in some amounts that are, in a first approximation, proportional to the respective masses at t' . In practice this is implemented as follows. We find the first and second most massive predecessors M_1 and M_2 at t' of the halo M at t . We then compare the ratio N_2/N_1 with the threshold Δ_m , where N_1 and N_2 are the number of particles in haloes M_1 and M_2 , respectively, with which these two predecessors contribute to the final halo M . When $N_2/N_1 > \Delta_m$, we consider that M formed in a major merger between t' and t and identify the two predecessors M_1 and M_2 as the progenitors which were destroyed in the event. On the contrary, when $N_2/N_1 \leq \Delta_m$ we consider that M is the result of the evolution by accretion of the most massive predecessor M_1 .

We must also assess whether a halo with mass M' at an output time t' was destroyed in a major merger *before the next output time* t or, alternatively, has evolved by accretion from t' to t . The procedure followed in this case is similar to that explained above. We find the set of haloes where the particles in M' end up at the later time t and select from this set the halo M that contains the greatest number of particles originally in M' . This halo is identified as the successor of M' . (When the successor of M' had less than 50% of its particles, then M' was discarded from our sample of putative haloes since it was not stable enough.) After identifying the successor M at t of M' at t' , we find the most massive predecessors of M at t' . There are then two possibilities: 1) M' is not the most massive predecessor of M , in which case M' has certainly been captured by a more massive halo between t' and t , being destroyed in the event; and 2) M' is the most massive predecessor of M , in which case we must identify the second most massive predecessor of M to assess, as explained above, whether M was formed (and M' destroyed) between t' and t or M' has evolved into M by accretion.

Following these prescriptions we can readily compute the fraction of haloes within a given mass bin which were formed or destroyed at some moment between two consecutive output times of the simulation. We can also identify haloes evolving by accretion and compute their mass evolution along a series of discrete times. Finally, we can identify the two progenitors of a halo and estimate its formation (or destruction) time.

4 RESULTS

4.1 Formation, destruction, and mass accretion rates

To evaluate the empirical formation rate we compute the fraction of haloes in a mass bin formed between two consecutive output times t_{k-1} and t_k and divide it by $\log(t_k/t_{k-1})$. This gives an estimate of the product $r^f(\tilde{M}, t_k)t_k$, where \tilde{M} is the central value of the normalized mass bin at t_k . Similarly, the destruction rate is evaluated by computing the fraction of haloes in a mass bin at t_k which are destroyed in a major merger between the consecutive output times t_k and t_{k+1} divided by $\log(t_{k+1}/t_k)$ which gives an estimate of the product $r^d(\tilde{M}, t_k)t_k$. In both cases, we average the results obtained from all pairs of consecutive output times by weighting their contribution in proportion to the number of haloes found in the corresponding normalized mass bin. The statistical error of this combined value is estimated as the weighted averaged Poisson errors of the values corresponding to each pair of consecutive output times.

To estimate the mass accretion rate, we first determine the set of haloes in a given mass bin at t_k that are not destroyed (i.e., which evolve by accretion) between t_k and t_{k+1} . Then, the average mass increase from t_k to t_{k+1} of haloes in such a set normalized to $M_*(t_k)$ and divided by $\log(t_{k+1}/t_k)$ yields an estimate of $[dM/d\log(t)]/M_*$, or equivalently, an estimate of the dimensionless quantity $r_{\text{mass}}^a(M, t_k)t_k/M_*(t_k)$, as we wanted. Finally, we average the results obtained for different times t_k in the same way as for the formation and destruction rates. For the error associated with this average, we take the weighted averaged r.m.s. mass increment of haloes in the mass bin divided by the square root of the total number of haloes in the bin.

Note that, in practice, the empirical time-derivatives that give the different growth rates are estimated by means of the finite increment approximation. Unfortunately, the size of the logarithmic time-increment used cannot be chosen arbitrarily small since the minimum available value is fixed by the output time step of the simulation. To check the finite increment approximation we present the results obtained using two different logarithmic time-increments: one equal to the output time step of the simulation (Fig. 3) and the other equal to two output time steps (Fig. 4). As can be seen, there is an excellent agreement between the theoretical and empirical growth rates for the whole range of halo masses that can be examined (almost four decades). The very slight deviations that can be detected (as in the case of the destruction rate) increase with increasing time-increments, which strongly suggests that they are caused by the finite-increment approximation.

The impressive agreement between theory and simulations is so far not surprising since the growth rates analysed were computed, after distinguishing between major and minor mergers, from the Lacey–Cole merger rate (LC93) which itself is in excellent agreement with N -body simulations (LC94). These results confirm, however, the overall consistency of the MPS prescriptions and the correctness of the practical procedure used to identify the formation and destruction of haloes in the simulations.

4.2 Accretion tracks

When comparing simulated and theoretical accretion tracks we are concerned with two main aspects: first, whether the real accretion tracks of individual haloes arising from random minor mergers substantially deviate from the theoretical track, in other words, whether the diffusion of real accretion tracks is important, and second, whether the theoretical accretion track is a good estimate of the *average* mass evolution followed by haloes between two consecutive major mergers, i.e., whether the diffusion is symmetric with regard to the theoretical mean track.

For each individual halo with M_i at t_i which does not satisfy the condition of an imminent major merger, we identify its successor at the next output time, and repeat the same procedure starting with this successor. We iterate the process until a successor is destroyed in a major merger. In this way we can predict the evolution due to accretion of the quantity $M(t)/M_*(t_i)$ that corresponds to any particular halo by taking the masses $M(t)$ equal to the masses of the successors found along the series of respective output times $t_k > t_i$. Figure 5 shows, for the three universes analysed, the mass evolution due to accretion of randomly selected haloes with initial normalized masses at t_i (corresponding to different output times of the simulation) in the logarithmic bins around $\tilde{M} = 0.3$ and $\tilde{M} = 3.0$. For comparison, we plot the theoretical accretion tracks corresponding to the central and the two limiting masses in each initial bin. As can be seen, the tracks of the simulated haloes show the same trend as those predicted by the theory. The former are, of course, affected by small random deviations (some of them quite notable because of minor mergers close to Δ_m), but in general the diffusion is rather moderate, as expected, because of the high frequency of minor mergers (particularly of very small mass) acting continuously between consecutive output times. This is apparent from the slow increase with time of the scatter of true tracks around the mean. At the ending time in each plot corresponding to two typical survival times of haloes in the initial bin, more than 20–30% of the surviving simulated tracks still remain inside the theoretical tracks bracketing each bin. (These percentages correspond to the global samples, not the random subsamples plotted in Fig. 5).

From Figure 5 one can also see that the diffusion is slightly asymmetric. The departure of the empirical average track relative to that of the theoretical mean is towards small masses when $n = -2$, towards large masses when $n = 0$, and intermediate between the two when $n = -1$. None the less, these deviations are quite moderate at least until two survival times, the only exception being the most massive bin of the $n = 0$ case. Note that such a deviation begins to be marked when the evolving normalized mass approaches unity. This is in overall agreement with our previous results on the evidence of asymmetric diffusion drawn from Figure 2.

4.3 Distribution of formation times

To determine the formation time of a simulated halo we follow its accretion-driven evolution back in time until a major merger is reached. In practice this is done in the following way. For a halo of mass M at t_i equal to some output time t_k we identify its two most massive progenitors at t_{k-1} and check (as explained in Section 3) whether a major merger took place between t_{k-1} and t_k . When this is not the case, we repeat the procedure for the most massive predecessor of M at t_{k-1} . By iterating this process we can follow the evolution of the successive most massive predecessors until the condition for a major merger is fulfilled. We then take the geometric mean between the two consecutive output times bracketing the major merger event as the formation time of the original halo with M at t_i . In this way we can obtain the formation time of all haloes in a fixed mass bin at t_i . The total fraction of haloes formed at distinct time intervals divided by the logarithmic output time step of the simulation yields a direct estimate of the product $\Phi_f(M, t)t$. The results obtained for distinct values of t_i (corresponding output times of the simulation) are finally averaged by weighting each individual contribution according to the total number of haloes from which the distribution is calculated (only those reliable distributions drawn from at least 50 objects are considered). The uncertainty associated to each bin of formation times is given by the weighted averaged Poisson errors from individual distributions.

In Figure 6 we show the empirical formation time PDFs of haloes with three different masses at t_i compared with the MPS predictions for the three universes analysed. As can be seen, there is also very good agreement for the full ranges of time that can be examined from the simulations in each particular case. We remind that the MPS prediction assumes haloes following the theoretical mean accretion track. We therefore conclude that the small diffusion of accretion tracks (shown in Figure 5) has a negligible effect on these PDFs. This conclusion holds even for large masses and very small formation times (of about one hundredth of the reference time t_i) as reached in the case of $n = 0$, when the effects of diffusion are the most marked.

4.4 Distribution of progenitor masses

For any newly formed halo (i.e., satisfying the condition of a recent major merger) we can store the masses of its two most massive predecessors which, according to our definition in Section 3.2, are considered its two progenitors. In this way the empirical PDF of progenitor masses can be computed for haloes selected in a given normalized mass bin at various output times. These results are then averaged following the same procedure as described in the previous subsection to derive the empirical PDF of formation times. Error bars are also calculated in the same manner.

According to our practical identification of halo formation explained in Section 3.2, the mass ratio between the two most massive progenitors at formation is taken to be equal to the ratio N_1/N_2 between their respective number of particles at the previous output time that are found within the newly formed halo at the next output time. Likewise, the mass ratio at formation between any of these progenitors and the new halo is taken to be equal to the ratio $N_p/(N_1 + N_2)$ where N_p stands for N_1 or N_2 .

Therefore, given two progenitors at t contributing with N_1 and N_2 particles, respectively, to the mass of a halo formed between t and the next output time, we store the quantity

$$\frac{1}{1 + N_2/N_1} = \frac{N_1}{N_1 + N_2}, \quad (17)$$

which gives an estimate of the fraction of the halo mass at formation that arises from the primary progenitor at that time. The PDF of this quantity must be compared with the theoretical PDF of M_1/M ratios, $\Phi_p(M_1/M)$, which coincides with the PDF of primary progenitor masses $\Phi_p(M_1, M)$ multiplied by the mass M of the halo at formation. This comparison is shown in Figure 7; note that this PDF is independent of time. Once again, the agreement between theory and simulations is very good.

What is actually plot in Figure 7 deserves some extra explanation. From expressions (13) and (14) it can be proved that the function $\Phi_p(M_1, M)M$ has a very weak dependence on the spectral index n of the power law spectra of density fluctuations. Concretely, one has

$$M \Phi_p(M_1, M) = \frac{2x^{(n-9)/6}}{(1-x^{(n+3)/3})^{3/2}} \left[\int_{\Delta_m/(1+\Delta_m)}^{1/(1+\Delta_m)} \frac{\tilde{x}^{(n-9)/6}}{(1-\tilde{x}^{(n+3)/3})^{3/2}} d\tilde{x} \right]^{-1}, \quad (18)$$

with $x = M_1/M$. For any value of M , equation (18) yields less than 1% difference among the PDFs of primary progenitor masses predicted for the three values of n of the cosmologies considered here. Given the resolution used in Figure 7, the PDF of primary progenitor masses predicted by the MPS model for the three $n = 0, -1$, and -2 cases should overlap on one single curve. This is the reason why there is only one unique theoretical curve plotted on this occasion for the three cosmologies. In other words, the MPS model makes a very restrictive prediction which, as seen in Figure 7, is also fully confirmed by the results of N -body simulations for the overall range of primary progenitor masses covered by the distributions.

5 SUMMARY AND DISCUSSION

We have compared the theoretical predictions of the MPS model with the output of cosmological N -body simulations in three Einstein-de Sitter scale-free cosmologies. The comparison included all quantities that play a fundamental role in the new model and have no counterpart in the EPS theory, namely, the formation rate, the destruction rate, the mass accretion rate, the theoretical accretion track, and the PDFs of halo formation times and progenitor masses. Overall, agreement was very good, which proves the validity of the MPS model as a powerful analytic tool for describing the growth history of dark-matter haloes in hierarchical cosmologies. In addition, the MPS model has the important advantage of avoiding the shortcomings that are encountered when constructing Monte Carlo merger trees from the usual EPS model.

We emphasize that the agreement between theory and simulations shown here does not depend on the particular value of Δ_m used to establish the effective frontier between minor and major mergers (provided, of course, that the same value is adopted in both theory and simulations). The results shown throughout this paper to illustrate the behaviour of the model correspond to $\Delta_m = 0.7$, although equally good results are obtained for any other value for this parameter.

As pointed out by Kitayama & Suto (1996) and SSM (and more recently by other authors, e.g., RGS; Percival & Miller 1999; Percival, Miller & Peacock 2000; Cohn, Bagla & White 2001), the distinction between minor and major mergers is necessary to properly define the concepts of halo formation and destruction. This is the key element making it possible to derive, in the MPS model, analytical expressions for the PDFs of formation times and halo progenitor masses which cannot be consistently derived in the framework of the EPS model.

The fact that the exact location of the effective frontier between minor and major mergers is irrelevant for the agreement between theory and simulations seems to suggest that the only reason for introducing a consistent definition for halo formation and destruction is to solve the problems met by the EPS model when dealing with Monte Carlo merger trees. Actually, as shown by Manrique et al. (2001), the formation of haloes through major mergers and their subsequent evolution through accretion

determine their internal properties. Hence, the proper characterization of these events is necessary to have a consistent description of both the mass growth and structure of haloes. A new model of galaxy formation based on the MPS model is currently under development.

ACKNOWLEDGMENTS

We thank Shaun Cole and Cedric Lacey for sending us the data of their N -body simulations and, particularly, C. Lacey for suggesting the comparison between the MPS model and simulations. This work was supported by the DGI of Spain through project number AYA2000-0951. A. Raig, who was supported by an FPI grant from the MEC of Spain, thanks the staff of TAC in Denmark for their hospitality during his stay at the beginning of this work.

REFERENCES

- Avila-Reese V., Firmani C., 1998, *ApJ*, 505, 37
 Bond J. R., Cole S., Efstathiou G., Kaiser N., 1991, *ApJ*, 379, 440
 Bower R. J., 1991, *MNRAS*, 248, 332
 Cavaliere A., Menci N., Tozzi P., 1999, *MNRAS*, 308, 599
 Cohn J. D., Bagla J. S., White M., 2001, *MNRAS*, 325, 1053
 Cole S., Aragón-Salamanca A., Frenk C. S., Navarro J. F., Zepf S. E., 1994, *MNRAS*, 271, 781
 Cole S., Lacey C. G., Baugh C. M., Frenk C. S., 2000, *MNRAS*, 319, 168
 Efstathiou G., Davis M., Frenk C. S., White S. D. M., 1985, *ApJS*, 57, 241
 González-Casado G., Raig A., Salvador-Solé E., 1999, in Giuricin G., Mezzetti M., Salucci P., eds, *ASP Conf. Ser. Vol. 176, Observational Cosmology: The Development of Galaxy Systems*. Astron. Soc. Pac., San Francisco, p. 438
 Gross M. A. K., Somerville R. S., Primack J. R., Holtzman J., Klypin A. A., 1998, *MNRAS*, 301, 81
 Jenkins A., Frenk C. S., White S. D. M., Colberg J. M., Cole S., Evrard A. E., Couchman H. M. P., Yoshida N., 2001, *MNRAS*, 321, 372
 Kauffmann G., White S. D. M., 1993, *MNRAS*, 261, 921
 Kauffmann G., White S. D. M., Guiderdoni B., 1993, *MNRAS*, 264, 201
 Kauffmann G., Colberg J. M., Diaferio A., White S. D. M., 1999, *MNRAS*, 303, 188
 Kitayama, T., Suto, Y., 1996, *MNRAS*, 280, 638
 Lacey C., Cole S., 1993, *MNRAS*, 262, 627 (LC93)
 Lacey C., Cole S., 1994, *MNRAS*, 271, 676 (LC94)
 Lacey C., Guiderdoni B., Rocca-Volmerange B., Silk J., 1993, *ApJ*, 402, 15
 Lee J., Shandarin S. F., 1998, *ApJ*, 500, 14
 Manrique A., Salvador-Solé E., 1996, *ApJ*, 467, 504
 Manrique A., Raig A., Solanes J. M., González-Casado G., Stein P., Salvador-Solé E., 1998, *ApJ*, 499, 548
 Manrique A., Salvador-Solé E., Raig A., 2001, *MNRAS*, submitted
 Navarro J. F., Frenk C. S., White S. D. M., 1997, *ApJ*, 490, 493 (NFW)
 Nulsen P. E. J., Fabian A. C., 1997, *MNRAS*, 291, 425
 Percival W. J., Miller L., 1999, *MNRAS*, 309, 823
 Percival W. J., Miller L., Peacock J. A., 2000, *MNRAS*, 318, 273
 Press W. H., Schechter P., 1974, *ApJ*, 187, 425
 Raig A., González-Casado G., Salvador-Solé E., 1998, *ApJ*, 508, L129 (RGS)
 Roukema B. F., Peterson B. A., Quinn P. J., Rocca-Volmerange B., 1997, *MNRAS*, 292, 835
 Salvador-Solé E., Solanes J. M., Manrique A., 1998, *ApJ*, 499, 542 (SSM)
 Salvador-Solé E., Manrique A., González-Casado G., Solanes J. M., Bruzual G., 2001, *Ap&SS*, in press
 Sheth R. K., Tormen G., 1999, *MNRAS*, 308, 119
 Sheth R. K., Mo H. J., Tormen G., 2001, *MNRAS*, 323, 1
 Somerville R. S., Kolatt T. S., 1999, *MNRAS*, 305, 1
 Somerville R. S., Primack J. R., 1999, *MNRAS*, 310, 1087
 Somerville R. S., Lemson G., Kolatt T. S., Dekel A., 2000, *MNRAS*, 316, 479
 Tormen G., 1998, *MNRAS*, 297, 648
 van Kampen E., Jimenez R., Peacock J. A., 1999, *MNRAS*, 310, 43

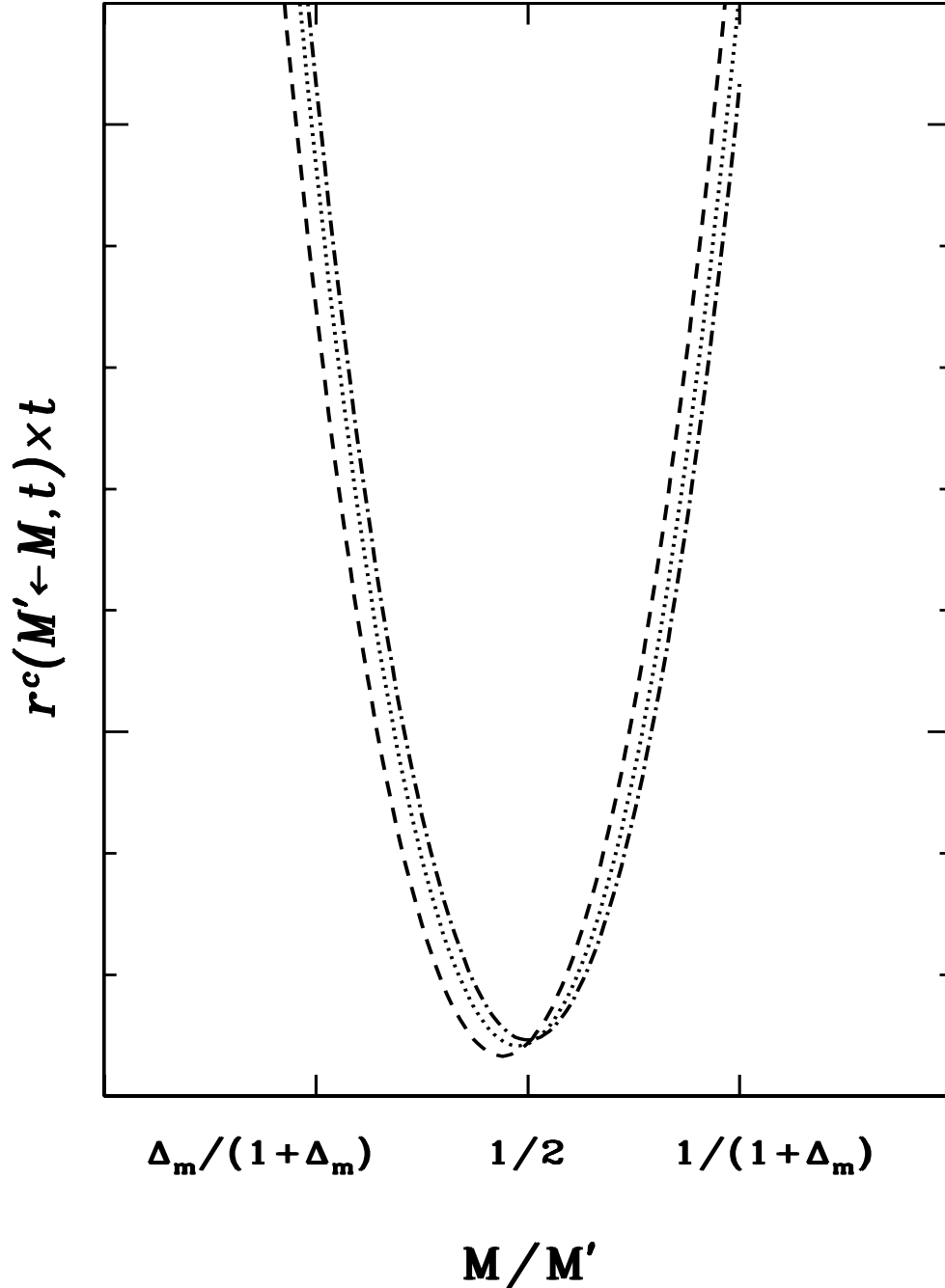


Figure 1. Shape around $M'/2$ of the instantaneous capture rate, in arbitrary units, for $M' = M_*$. The captured mass M on the x -axis is normalized to M' so to have time-independent results. The curves correspond to the three cosmologies analysed ($n = -2$ in dashed line, $n = -1$ in dotted line, and $n = 0$ in dot-dashed line). A similar behaviour is found for any other value of M' .

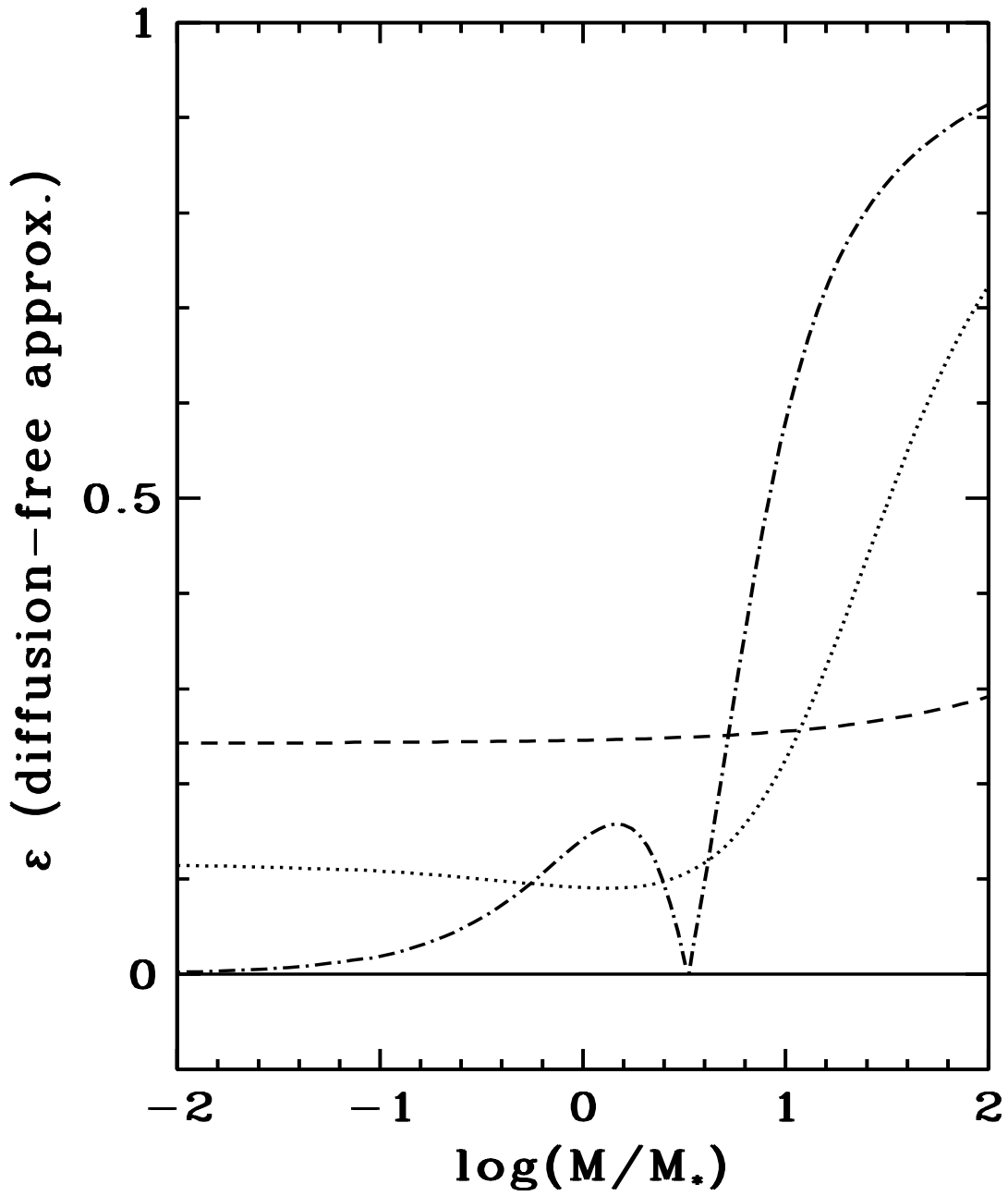


Figure 2. Absolute value of the relative difference, as a function of halo mass, between the formation rates estimated from condition (12) and equation (6) for the three scale-free cosmologies analysed (same line coding as in Fig. 1). Halo masses on the x -axis are normalized to the characteristic mass M_* defined in equation (15) so as to have time-independent results.

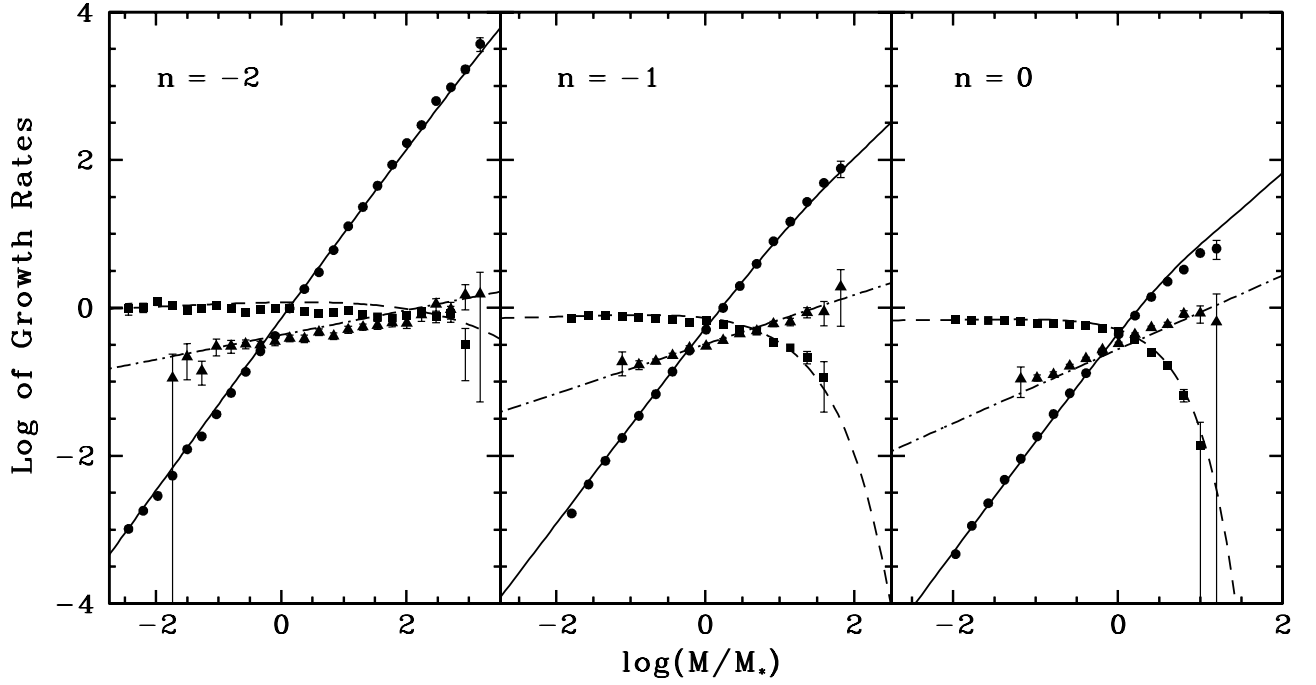


Figure 3. Comparison between the growth rates predicted by the MPS model (lines) and drawn from the simulations (symbols) using a logarithmic time-increment equal to the output time step of the corresponding simulation for the three scale-free cosmologies analysed: $n = -2$ (left panel), $n = -1$ (central panel), and $n = 0$ (right panel). Theoretical destruction rates are in dashed lines (squares for the empirical results), formation rates in dot-dashed lines (triangles), and mass accretion rates in solid lines (circles). Error bars and symbols have similar sizes except at both mass ends.

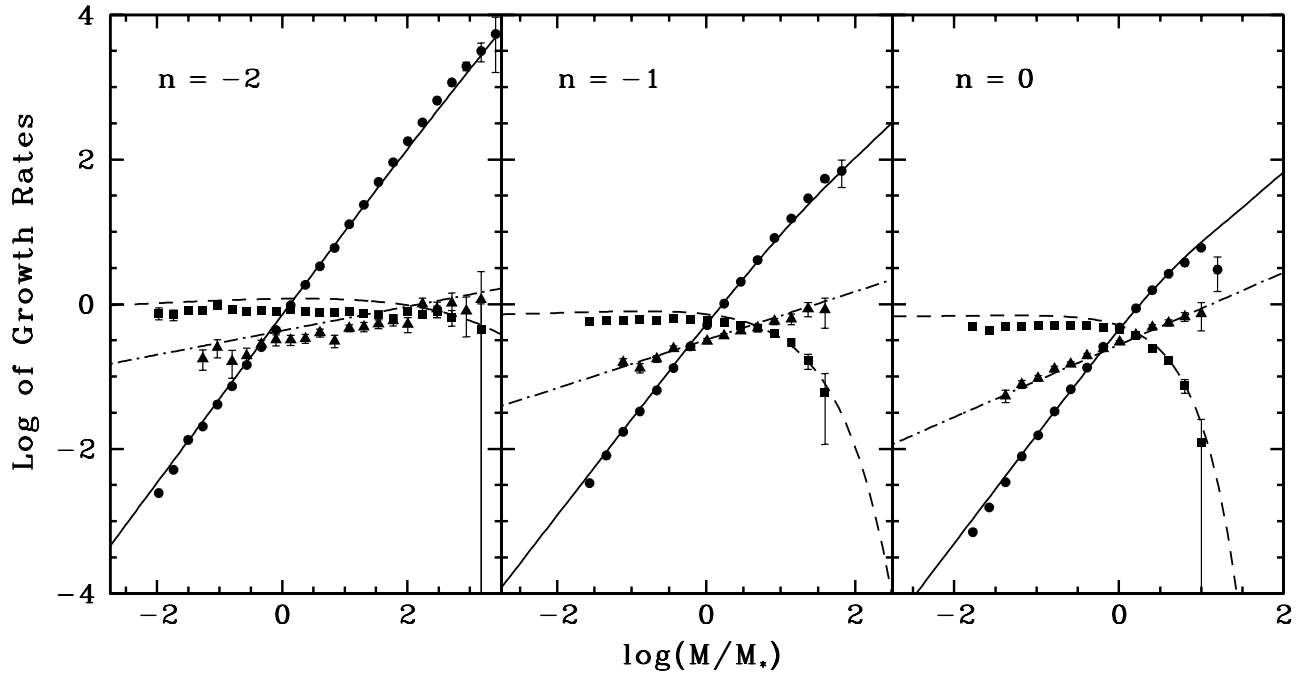


Figure 4. Same as Figure 3 for a logarithmic time-increment equal to two output time steps of each simulation.

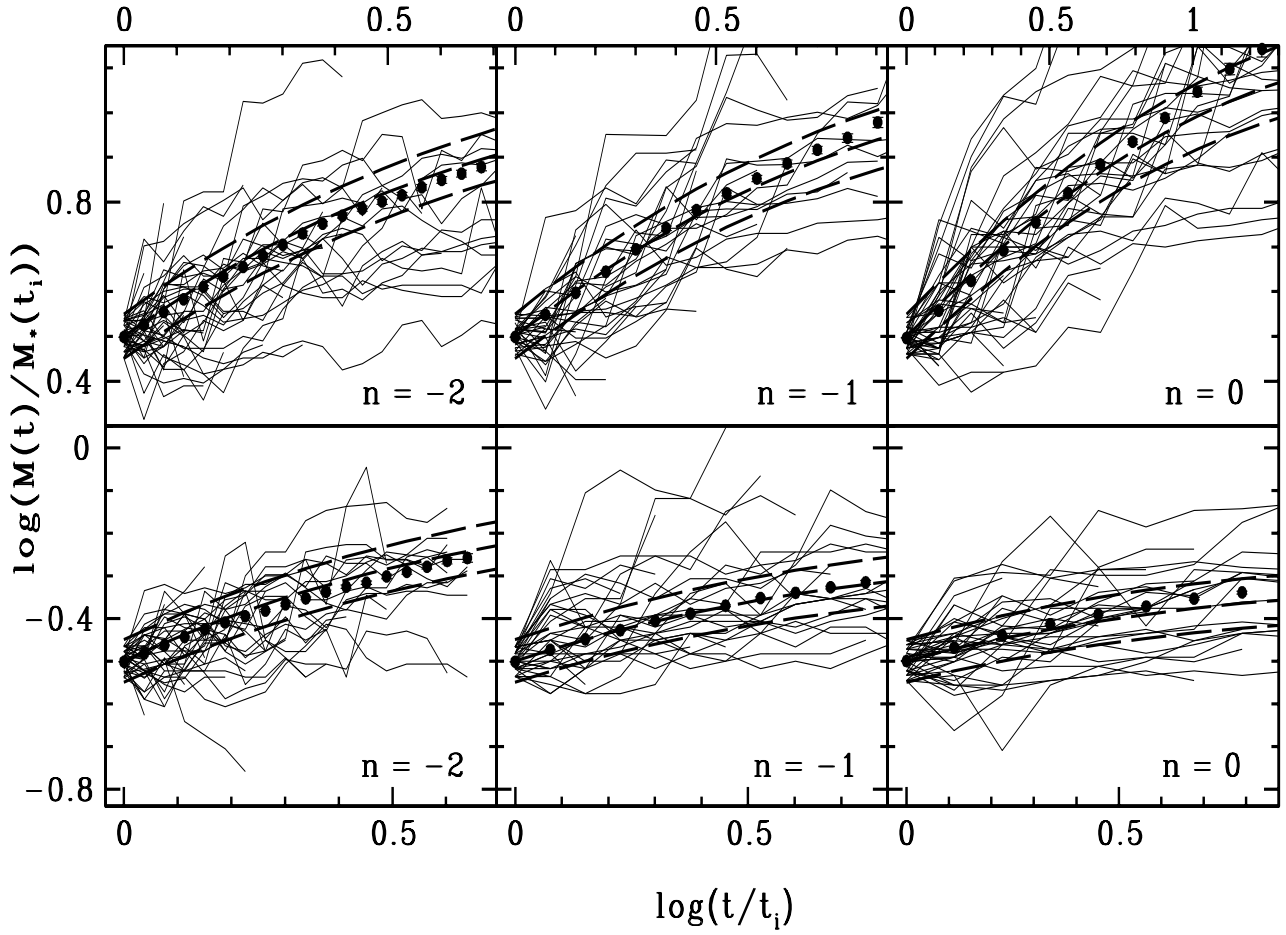


Figure 5. Accretion tracks followed by randomly selected haloes with initial masses at t_i in logarithmic bins of 0.1 width centred on $M = 0.3M_*$ (lower panels) and $M = 3.0M_*$ (upper panels) in the three cosmologies analysed. In thin lines tracks drawn from simulations. In thick dashed lines the theoretical accretion tracks for the central mass as well as for the two masses bracketing each initial mass bin. Dots show the time evolution of the average mass of simulated haloes initially in each mass bin. Error bars are much smaller than the dot size.

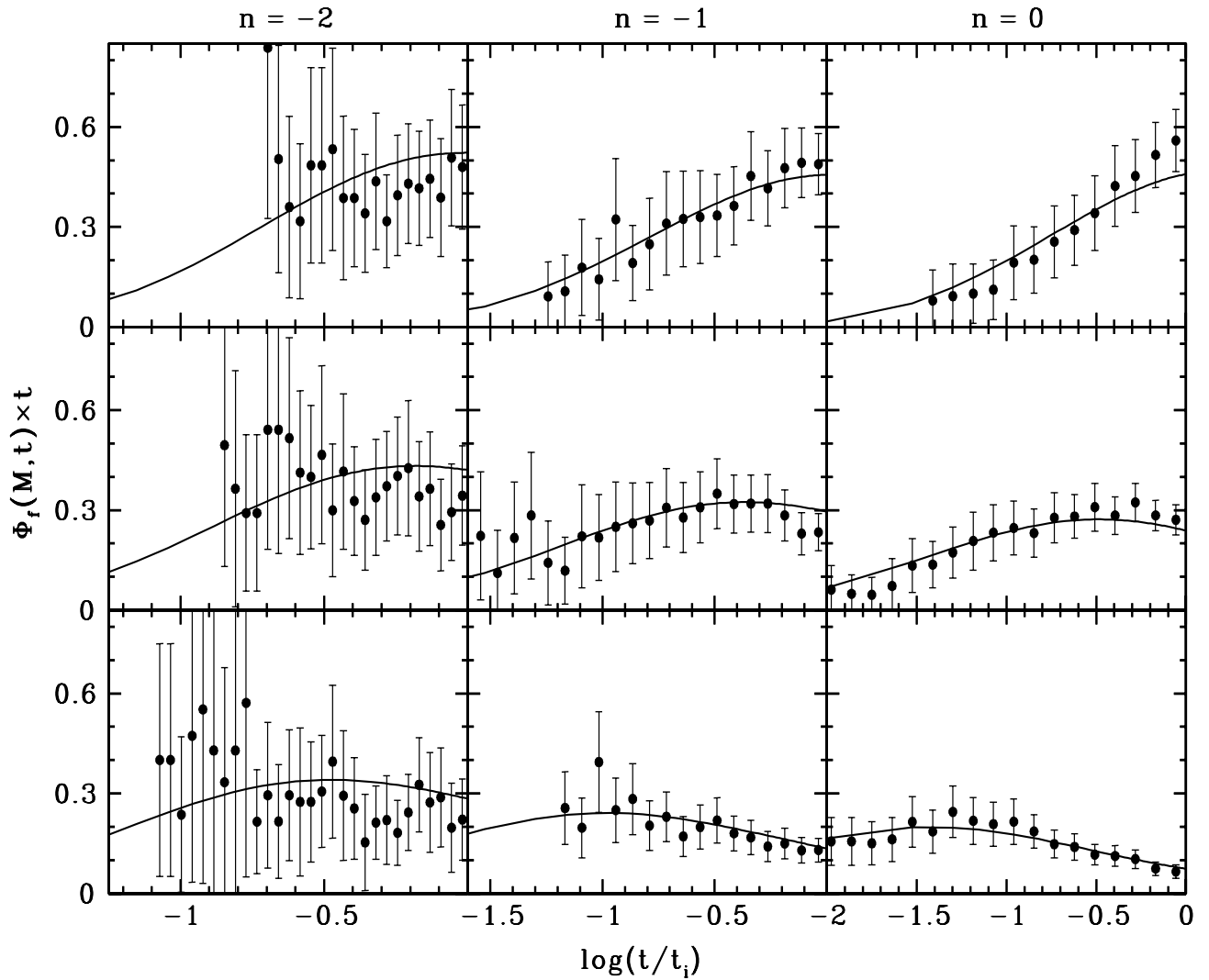


Figure 6. Comparison between theoretical (solid lines) and empirical (dots) formation time PDFs for haloes of three distinct masses ($2.8 M_*$ in the top panels, $0.7 M_*$ in the middle panels, and $0.07 M_*$ in the bottom panels) in the three cosmologies analysed.

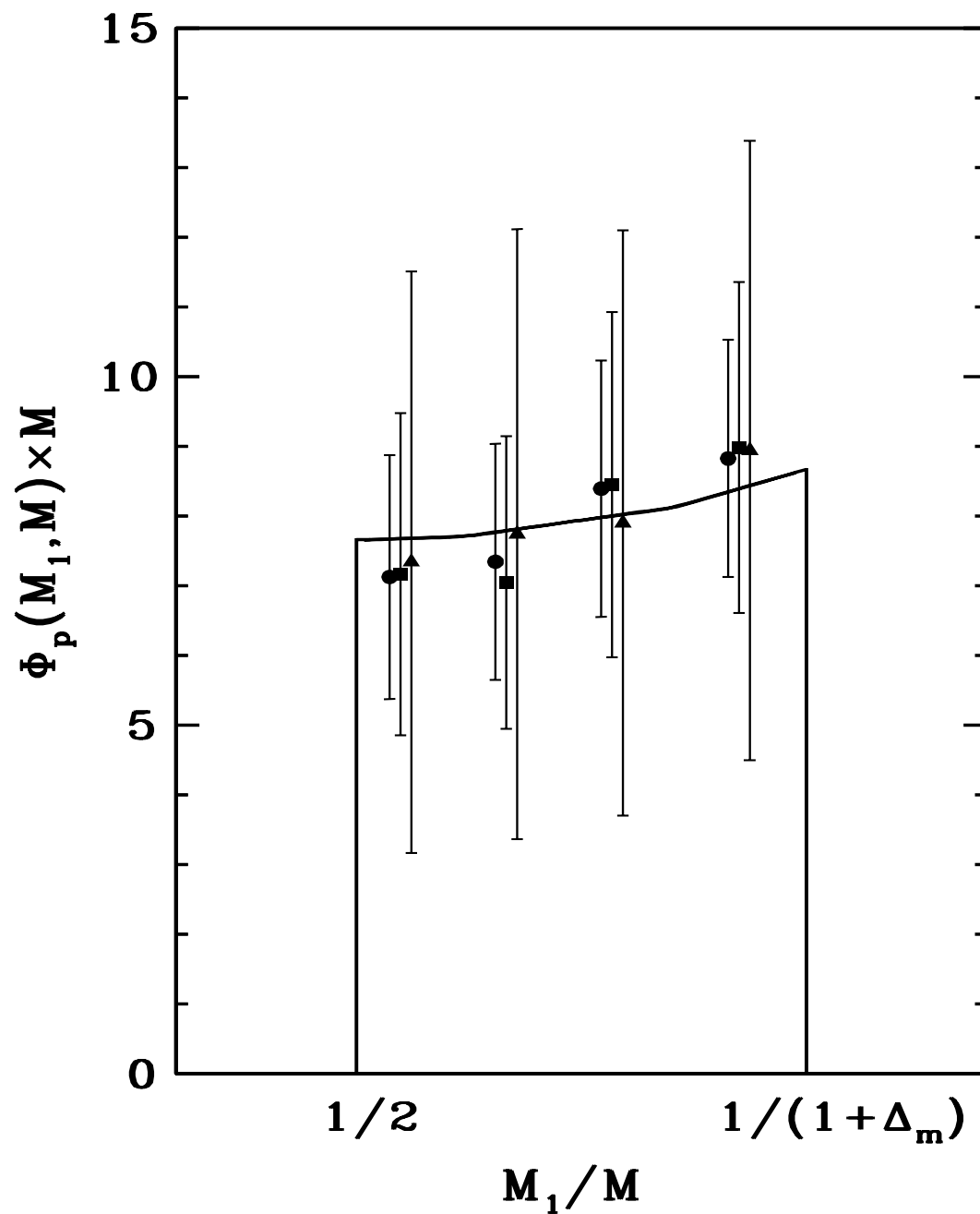


Figure 7. Comparison between theoretical (solid line) and empirical (symbols) PDFs of primary progenitor masses M_1 for a halo with arbitrary mass M at formation in the three cosmologies analysed (triangles for $n = -2$, squares for $n = -1$, and circles for $n = 0$). For clarity, we have shifted the abscissae of the empirical points corresponding to the $n = -2$ and $n = 0$ cosmologies slightly, their true location coinciding with those of the $n = -1$ cosmology.